

# Oscillatory Magneto-Thermopower and Resonant Phonon Drag in a High-Mobility 2D Electron Gas

Jian Zhang,<sup>1</sup> S. K. Lyo,<sup>2</sup> R. R. Du,<sup>1</sup> J. A. Simmons,<sup>2</sup> and J. L. Reno<sup>2</sup>

<sup>1</sup>*Department of Physics, University of Utah, Salt Lake City, Utah 84112*

<sup>2</sup>*Sandia National Laboratories, Albuquerque, New Mexico 87185*

(Dated: October, 10, 2003)

Experimental and theoretical evidence is presented for new low-magnetic-field ( $B < 5$  kG)  $1/B$ -oscillations in the thermoelectric power of a high-mobility GaAs/AlGaAs two-dimensional (2D) electron gas. The oscillations result from inter-Landau-Level resonances of acoustic phonons carrying a momentum equal to twice the Fermi wavenumber at  $B = 0$ . Numerical calculations show that both 3D and 2D phonons can contribute to this effect.

PACS numbers: 73.50.Rb, 73.40.-c, 72.20.Pa

Thermoelectric power (TEP) of a two-dimensional electron gas (2DEG) reflects the electron density of states, scattering dynamics, and electron-phonon interactions. Phonon scattering and consequently the TEP are particularly important in GaAs/Al<sub>x</sub>Ga<sub>1-x</sub>As heterostructures owing to the strong electron-lattice coupling in these materials. The TEP experiments in the following two limits of the magnetic field ( $B$ ) have been widely pursued [1, 2, 3, 4, 5, 6, 7, 8, 9, 10] and the phenomena in these regimes are relatively well-understood [11, 12, 13, 14, 15]. At  $B = 0$ , the TEP ( $S_0$ ) shows a power-law, e.g.,  $T^{3-4}$ , temperature dependence above  $T \sim 0.3$  K, indicating that the phonon drag mechanism dominates and the electron-diffusion effect is relatively weak. In the regime of a high field ( $B > 10$  kG), Shubnikov de-Haas (SdH) oscillation and quantum Hall effect have been observed in TEP [9, 10]. The peak amplitude of the TEP are found to be greater than the predicted values of the diffusion TEP by 2 orders of magnitude, but consistent with the phonon-drag TEP. Most of the above experimental data at  $B = 0$  and at relatively high fields have been successfully explained quantitatively by theories based on the phonon drag TEP.

On the contrary, little is known experimentally about the TEP in the regime of a weak magnetic field, where many Landau levels (LLs) are occupied by electrons with large quantum numbers  $n \gg 1$  at the Fermi level, and electronic transport is generally treated semiclassically. This regime is characteristically distinct for the following reasons. 1) The Fermi wave length is much shorter than the magnetic length  $l_B = \sqrt{\hbar/eB}$  (i.e.,  $2k_F l_B \gg 1$ ), and a momentum selection rule governs the scattering of electron guiding centers. In particular,  $2k_F$  scattering is strongly enhanced, giving rise to the low  $B$  resonance phenomena [16, 17] in this regime. 2) Acoustic phonons in GaAs have suitable energies, and in combination with 1) can participate in inter-LL scattering. This is dramatically different from the regime of higher  $B$ , where intra-LL scattering dominates and inter-LL scattering is negligible at low temperatures[14]. Elastic intra-LL scat-

tering is important for LL broadening.

In this Letter, we report low- $B$  TEP oscillations observed in a high-mobility 2DEG in GaAs/Al<sub>x</sub>Ga<sub>1-x</sub>As heterostructures. The oscillations are periodic in  $1/B$  with the peak positions of  $B$  proportional to  $\sqrt{n_e}$ , or to the Fermi wavenumber  $k_F = \sqrt{2\pi n_e}$ , where  $n_e$  is the electron density. Characteristically, such oscillations appear in the temperature range 0.5 K - 1 K, and their amplitude increases with  $T$ . It will be shown that the TEP oscillations result from inter-LL cyclotron resonance promoted by resonant absorption of phonons carrying a  $2k_F$  in-plane momentum and an energy  $\ell\hbar\omega_c$  equal to the integer ( $\ell = 1, 2, \dots$ ) multiple of  $\hbar\omega_c = \hbar eB/m^*$ , which is the cyclotron energy with an effective mass  $m^*$ . 2D phonon modes propagating along the GaAs/Al<sub>x</sub>Ga<sub>1-x</sub>As interface and 3D phonons are responsible for the TEP oscillations. However, the contribution from 2D phonons is difficult to assess quantitatively because of the lack of electron-2D phonon interaction parameters. On the other hand, numerical calculations show that 3D phonons yield a substantial contribution to the oscillation and behave like 2D phonons for the  $2k_F$ -oscillation because  $q_z$  is restricted to small  $q_z \ll 2k_F$  at low temperatures due to the phonon occupation factor.

The TEP experiments were performed using a sorption pumped <sup>3</sup>He cryostat and a superconducting solenoid, with the B axis always oriented perpendicular to the 2DEG plane. The samples used here are made from GaAs/Al<sub>0.3</sub>Ga<sub>0.7</sub>As heterostructures grown by molecular beam epitaxy on the (001) GaAs substrate. At low temperature ( $T \sim 1$  K), the  $n_e$  and the mobility,  $\mu$ , can be varied using a red light-emitting diode (LED). Without LED (saturate LED) the  $n_e$  (in unit of  $10^{11}\text{cm}^{-2}$  throughout this paper)  $\sim 1.33$  (2.03) and  $\mu \sim 2 \times 10^6$  ( $3 \times 10^6$ )  $\text{cm}^2/\text{Vs}$ . To make TEP measurement, a specimen of dimension 8 mm  $\times$  2 mm was first cleaved from the wafer and a Hall bar mesa (width 0.5 mm) was then chemically wet-etched from it by optical lithography. Heat sink to a copper post (0.3 K) was achieved by indium soldering at one end of the specimen. A strain

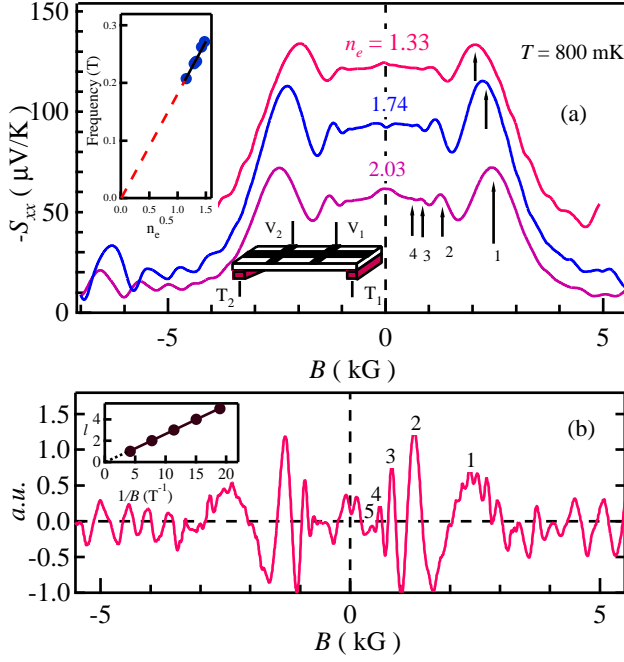


FIG. 1:  $-S_{xx}$  traces are shown for three densities  $n_e$  of 1.33, 1.74, and 2.03 in units of  $10^{11}\text{cm}^{-2}$ , respectively; arrows indicate the maxima for  $l=1, 2, 3, 4$  and the shift of the primary ( $l=1$ ) peak with increasing  $n_e$ . In the lower figure, the second derivative against  $B$  for the high-density trace is shown; the numbers mark the oscillation peaks. Inset shows that oscillations are periodic in  $1/B$ .

gauge was glued to the other end of the specimen by Ag paint and was used as a heater to create a temperature gradient ( $\nabla T$ ) along the Hall bar direction. Two calibrated  $\text{RuO}_2$  chip sensors were glued by epoxy 2850FT [18] on the back of the specimen and used to measure the  $\nabla T$  along the sample. Electrical leads were made with 38 gauge manganin wires, whose low thermal conductance ensures a negligible heat leak to the  $^3\text{He}$  liquid. The whole system was sealed in a vacuum can made of epoxy [19]. The vacuum can including the copper cold sink were immersed in the  $^3\text{He}$  liquid.

The TEP  $S_{xx}$  is defined by  $\nabla V_{xx} = S_{xx} \nabla T$ , with the quantities measured in the following manner. A low frequency ( $f_0 = 2.7\text{Hz}$ ) ac voltage was applied to the heater and the  $T_1, T_2$  (see inset, Fig. 1) were measured using the  $\text{RuO}_2$  sensors and a AC bridge. The  $V_{xx}$  induced by the thermo-gradient was measured by lock-in method at the frequency of  $2f_0 = 5.4\text{Hz}$ . Both the  $T$  and voltage gradients were calculated using the dimensions given by the specimen.

In Fig. 1(a), we show the low field magneto-TEP measured at 800 mK, for three electron densities. These traces reveal strong new oscillations appearing at  $B < 3\text{ kG}$ , where SdH oscillations are relatively weak. For example, up to four maxima can be clearly seen in the trace

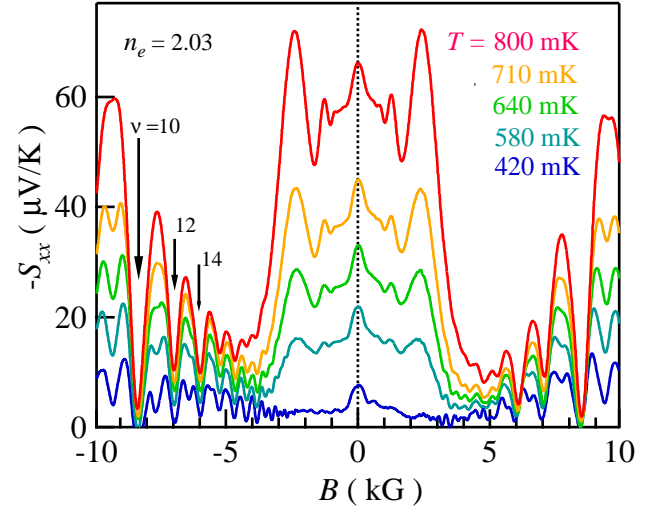


FIG. 2:  $-S_{xx}$  (for  $n_e = 2.03 \times 10^{11}\text{cm}^{-2}$ ) traces at different temperatures show that the low field oscillations become stronger as  $T$  increases.

of  $n_e = 2.03$ . The arrows close to the traces indicate the maxima (indexed as  $l = 1, 2, 3, 4$ ). A second derivative with respect to  $B$ ,  $-d^2 S_{xx}/dB^2$ , for the  $n_e = 2.03$  is plotted in (b), together with a fan diagram (inset) showing the linear relation between the order,  $l$ , and the inverse  $B$ . We conclude from all three traces that the TEP oscillations are periodical in  $1/B$ . Moreover, the peak positions of  $B$  scales with  $\sqrt{n_e}$ , as shown in the inset of Fig. 1(a). This behavior is distinct from that of SdH which scales with  $n_e$ , but consistent with the characteristics of a class [16, 17] of weak  $B$  oscillations originating from cyclotron resonance with a  $2k_F$  momentum transfer.

The TEP oscillations exhibit a remarkable  $T$  dependence, which, as will be shown later, can be attributed to inter-LL scattering by acoustic phonons. As an example, Fig. 2 shows the TEP data for  $n_e = 2.03$  at a  $T$  range from 420 mK to 800 mK. Note that the TEP oscillation can be discerned at  $T$  as low as 300 mK for our experiment. With increasing  $T$ , the TEP signal increases dramatically, both at  $B = 0$ , and at  $B < 5\text{ kG}$ . The TEP at  $B = 0$ ,  $S_0$ , is well understood as due to phonon drag. As will be shown, the  $S_0$  is power-law dependent in this experiment. As  $T$  rises, the TEP oscillation amplitude increases faster than  $S_0$ . This fact indicates that inter-LL scattering is dominant in the TEP oscillations observed here, since inter-LL scattering mechanism leads to an exponential rather than a power-law  $T$  dependence. As the cyclotron energy increases, the inter-LL scattering regime with an exponential-law  $T$ -dependence disappears and only the intra-LL-scattering SdH regime with a power-law  $T$ -dependence prevails[14]. Indeed, at higher temperatures,  $T \geq 800\text{ mK}$ , the TEP oscillations become the dominating feature in TEP measurement at low field.

We now turn to a quantitative analysis for  $S_0$  and the

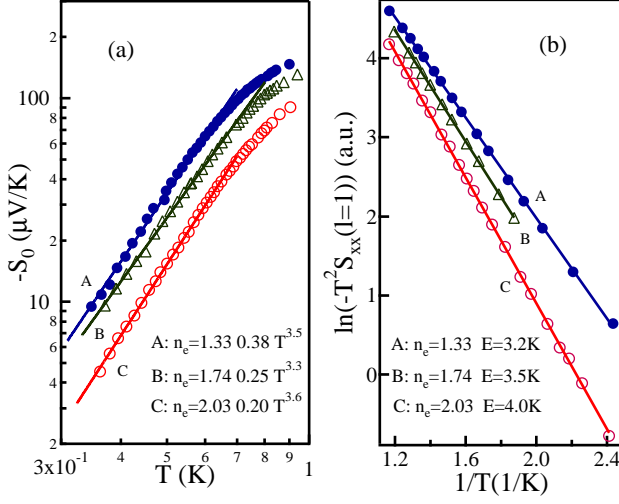


FIG. 3: The left figure shows the  $T$  dependence of the TEP at zero field ( $S_0$ ), for three densities. The solid lines represent  $T^3$  temperature dependence. The right figure shows the  $T$  dependence of the TEP at primary oscillation maxima ( $l = 1$ ), for the three corresponding densities. The  $E$  is the fitted value for the phonon energy at  $l = 1$ .

TEP oscillations. In Fig. 3(a), we plot  $S_0$  vs.  $T$  for three densities. All data show a power-law dependence on  $T$ , with an exponent between 3 and 4. This observation confirms quantitatively that the TEP at  $B = 0$  is by the phonon drag mechanism [9]. The  $T$ -dependent amplitude of the first peak ( $l = 1$ ) is presented in Fig. 3(b). It is worth noting that the data strongly deviates from a power-law, but can be fitted by a modified exponential relation  $S_{xx} \sim \exp(-E/k_B T)/T^2$ , predicted by equation (1). From the slope of the fit we arrive at the activation energies  $E \sim 3.2$  K, 3.5 K, 4.0 K, respectively for the three densities, which are somewhat smaller than  $\hbar\omega_c \sim 4.0$  K, 4.4 K, 4.8 K due to the LL broadening. These data strongly support the interpretation of a resonant phonon drag mechanism being the origin of the TEP oscillations.

In principle, both 3D and 2D phonons can contribute to the resonant phonon drag mechanism responsible for the oscillations. We start by considering the 3D case, in the following, on a more general ground. Qualitatively, the 2D case can be reduced from the 3D case.

We begin with the formula for the phonon drag TEP in a magnetic field derived by Lyo [14]; a similar formulism was given by Kubakaddi and Butcher [11]. The TEP is obtained for a unit volume:

$$S_{xx} = \frac{-k_B \hbar}{e \nu (k_B T)^2} \sum_{s\mathbf{q}} \sum_{n, n'} u_s \Lambda_{s\mathbf{q}} q_y^2 n_{s\mathbf{q}} |V_{s\mathbf{q}}|^2 \Delta_z(q_z) \Delta_{n, \ell}(q_{\parallel}) \times \int d\varepsilon \rho_n(\varepsilon) \int d\varepsilon' \rho_{n'}(\varepsilon') f(\varepsilon) [1 - f(\varepsilon')] \delta(\varepsilon + \hbar\omega_{s\mathbf{q}} - \varepsilon'), \quad (1)$$

where  $\nu = \pi n_e l_B^2$  is the filling factor for spin-degenerate LLs,  $\Lambda_{s\mathbf{q}}$  the phonon mean-free-path,  $n_{s\mathbf{q}}$  the boson function,  $f(\varepsilon)$  the Fermi function,  $u_s$  the sound velocity for the mode  $s$ ,  $\rho_n$  the spectral function for the LLs, and  $\Delta_z(q_z)$  is the conservation factor for  $q_z$  [14]. The square of the absolute value of the electron-phonon matrix element  $|V_{s\mathbf{q}}|^2$  is proportional to the in-plane-momentum conservation factor:

$$\Delta_{n, \ell}(q_{\parallel}) = \frac{n!}{(n + \ell)!} \chi^\ell e^{-\chi} [L_n^\ell(\chi)]^2, \quad \chi = \frac{(q_{\parallel} l_B)^2}{2}, \quad (2)$$

which has a sharp principal maximum near  $\chi = 4n$ , namely, near the in-plane momentum transfer  $q_{\parallel} \simeq 2k_F$  for  $n \gg 1$ ,  $\ell$  in view of  $\varepsilon_F \simeq n \hbar \omega_c$  [16, 20]. In Eq. (2),  $L_n^\ell(\chi)$  is the associated Laguerre polynomial and  $n' = n + \ell$  is the larger of  $n$  and  $n'$ . The phonon occupation factor restricts  $q_z$  to small values  $q_z \ll 2k_F$  for this resonance at low temperatures. There are other secondary peaks below the main peak for  $\Delta_{n, \ell}(q_{\parallel})$ . To reduce the computing time, we approximate the spectral density function  $\rho_n(\varepsilon)$  by a rectangular distribution with a full width  $2\Gamma$  centered at the LL energy  $\varepsilon_n = \hbar\omega_c(n + 1/2)$  and take  $\Gamma = 0.2$  meV for numerical evaluation.

The calculated TEP is plotted as a function of  $B$  in Fig. 4, for  $\Lambda_{s\mathbf{q}} = 2$  mm and respectively for three densities,  $2.03, 1.74$ , and  $1.33 \times 10^{11} \text{ cm}^{-2}$  employing field-free screening for the electron-phonon interaction. Other parameters are well-known and are given in Ref. [14]. The TEP is proportional to the phonon mean-free-path  $\Lambda_{s\mathbf{q}}$ , which is basically an adjustable parameter. At low temperatures considered here,  $\Lambda_{s\mathbf{q}}$  is determined by boundary scattering and is expected to be of the order of the smallest sample dimension  $\sim 2$  mm. It is seen that the  $\ell = 1, 2, 3, \dots$  peaks appear on top of the regular SdH oscillations which are from the phonons with  $q_{\parallel} < 2k_F$ . Larger  $\Gamma$  makes the peaks broader and the valleys shallower compared to the sharper structures obtained for  $\rho_n(\varepsilon) = \delta(\varepsilon - \varepsilon_n)$ . A, B and C traces display the TEP as a function of  $B$  for three densities  $n_e = 1.33, 1.74, 2.03 \times 10^{11} \text{ cm}^{-2}$  at 0.8 K. It is seen that there is an approximate scaling relationship between the peak positions of  $B$ , satisfying  $B \propto \sqrt{n_e}/\ell$ . This relationship is consistent with the inter-LL resonance phonon picture  $\hbar\omega_{2k_F} \simeq \ell \hbar e B / m^*$  in view of  $\omega_{2k_F} \propto k_F \propto \sqrt{n_e}$ , yielding reasonable agreement with experimental data. We also find  $S_{xx} \propto \exp(-E/k_B T)/T^2$  in agreement with Fig. 3(b) with  $E \propto \sqrt{n_e}$  close to the transverse  $2k_F$  phonon energy. Transverse phonons yield a dominant contribution ( $\sim 70\%$ ) through strong piezoelectric scattering at low temperatures. The calculated background TEP is much lower than the peaks compared with the data in Fig. 2 probably due to the simplistic non-self-consistent density of states employed in the present low- $B$  situation where the LLs are closely separated. Also, the magnitude of the calculated TEP keeps decreasing

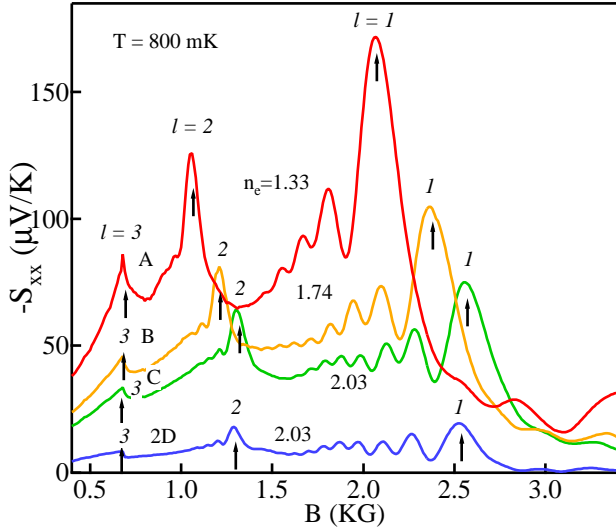


FIG. 4: Numerical calculation of the TEP at low fields based on the 3D phonon model (upper three curves). The bottom curve is an estimate from a 2D-phonon model. The primary oscillation maxima increase with  $T$ , decrease with increasing  $n_e$ . Their  $B$  positions shift to lower field with decreasing  $n_e$ .

as  $B$  approaches  $B = 0$  in contrast to the data: Below  $B < 0.4$  kG, the number of the LLs becomes very large ( $n > 100$ ), requiring a zero- $B$  formalism for a more accurate result.

The 2D phonon modes relevant in the GaAs/Al<sub>x</sub>Ga<sub>1-x</sub>As heterostructures are the leaky phonons [16, 21] with phonon wave vector component  $q_z = 0$  and  $q = q_{\parallel}$ . The TEP is again given by Eq. (1) with  $\Delta(q_z) \equiv 1$  with the summation on  $q_z$  replaced by the summation over the leaky modes. For a rough estimate, we take same  $|V_{sq}|$  with the effective sample volume given by  $\Omega = S\ell_p$ , where  $S$  is the cross section of the well and  $\ell_p$  is roughly the penetration depth of the mode. The result for the 2D phonons is compared with that of the 3D phonons in Fig. 4 for  $\ell_p = 200$  Å using a pair of longitudinal and transverse modes. The  $B$  dependence of  $S_{xx}$  from the 2D phonons in Fig. 4 is very similar to that from the 3D phonons except that it is slightly shifted to lower  $B$ .

In Fig. 3(a), the linear contribution  $S_0 \propto T$  from the electron-diffusion TEP is negligible at  $B = 0$ . This situation is similar to the data of Tieke, *et al.* [9], but different from the results of C. Ruf, *et al.* [22], in which the diffusive TEP is visible at 0.6K and the data deviate from the  $T^3$  slope at 0.6K.

A high-mobility sample is necessary to observe this low-field acoustic-phonon resonance. In high mobility samples, high LLs are not easily smeared out by impurity-scattering. We expect stronger and sharper  $2k_F$  oscillations for higher-mobility samples.

In conclusion, we have reported for the first time an

oscillatory TEP in a weak magnetic field, where inter-LL scattering is accessible by acoustic phonons. The observation of such oscillations confirms a generic  $2k_F$  momentum selection rule in electronic transport in a weak magnetic field where many LLs are occupied. Finally, it is found that while both 3D and 2D phonons cause qualitatively similar TEP oscillations in this regime, 3D phonons yield a substantial contribution to the oscillations to explain the data.

We acknowledge helpful conversations with Prof. R. Fletcher. S. K. L thanks Dr. D. E. Amos for his indispensable help with the computation. The work at the University of Utah was supported by NSF and by a DARPA-QuIST grant. Sandia is a multiprogram laboratory operated by Sandia Corporation, a Lockheed Martin Company, for the U.S. DOE under Contract No. DE-AC04-94AL85000.

- 
- [1] R. Fletcher, J. C. Maan, and G. Weimann, Phys. Rev. B. **32**, 8477 (1985).
  - [2] R. J. Nicholas, J. Phys. C: Solid State Phys. **18**, L695 (1985).
  - [3] J. S. Davidson, E. D. Dahlberg, A. J. Valois and G. Y. Robinson, Phys. Rev. B. **33**, 2941 (1986).
  - [4] R. Fletcher, J. C. Maan, K. Ploog and G. Weimann, Phys. Rev. B. **33**, 7122 (1986).
  - [5] R. Fletcher, M. D'Iorio, A. S. Sachrajda, R. Stoner, C. T. Foxon, and J. J. Harris, Phys. Rev. B. **37**, 3137 (1988).
  - [6] X. Ying, V. Bayot, M. B. Santos and M. Shayegan, Phys. Rev. B. **50**, 4969 (1994).
  - [7] U. Zeitler, R. Fletcher, J. C. Maan, C. T. Foxon, J. J. Harris, and P. Wyder, Surf. Sci., **305**, 91 (1994).
  - [8] V. Bayot, E. Grivei, H. C. Manoharan, X. Ying, and M. Shayegan, Phys. Rev. B. **52**, R8621 (1995).
  - [9] B. Tieke, R. Fletcher, U. Zeitler, M. Henini, and J. C. Maan, Phys. Rev. B. **58**, 2017 (1998).
  - [10] R. Fletcher, V. M. Pudalov, Y. Feng, M. Tsousidou, and P. N. Butcher, Phys. Rev. B. **56**, 12422 (1997).
  - [11] D. G. Cantrell and P. N. Butcher, J. Phys. C. **20**, 1985 (1987).
  - [12] S. K. Lyo, Phys. Rev. B. **38**, 6345 (1988).
  - [13] S. S. Kubakaddi, P. N. Butcher, and B. G. Mulimani, Phys. Rev. B. **40**, 1377 (1989).
  - [14] S. K. Lyo, Phys. Rev. B. **40**, 6458 (1989).
  - [15] M. J. Smith and P. N. Butcher, J. Phys.: Condens. Matter. **2**, 2375 (1990).
  - [16] M. A. Zudov, I. V. Ponomarev, A. L. Efros, R. R. Du, J. A. Simmons, and J. L. Reno, Phys. Rev. Lett. **86**, 3614 (2001).
  - [17] C. L. Yang, J. Zhang, R. R. Du, J. A. Simmons, and J. L. Reno, Phys. Rev. Lett. **89**, 076801 (2002).
  - [18] Stycast 2850FT, Emerson and Cuming Inc., Lexington, MA.
  - [19] Stycast 1266 A/B, Emerson and Cuming Inc., Lexington, MA.
  - [20] H. Scher and T. Holstein, Phys. Rev. **148**, 598 (1966).
  - [21] I. V. Ponomarev and A. L. Efros, Phys. Rev. B. **63**, 165305 (2001).

- [22] C. Ruf, H. Obloh, B. Junge, E. Gmelin, K. Ploog, and G. Weimann, Phys. Rev. B. **37**, 6377 (1988).